

# Vortex lattice transitions in cyclic spinor condensates

Ryan Barnett,<sup>1</sup> Subroto Mukerjee,<sup>2,3</sup> and Joel E. Moore<sup>2,3</sup>

<sup>1</sup>*Department of Physics, California Institute of Technology, MC 114-36, Pasadena, California 91125, USA*

<sup>2</sup>*Department of Physics, University of California, Berkeley, CA 94720 and*

<sup>3</sup>*Materials Sciences Division, Lawrence Berkeley National Laboratory, Berkeley, CA 94720*

(Dated: November 20, 2021)

We study the energetics of vortices and vortex lattices produced by rotation in the cyclic phase of  $F = 2$  spinor Bose condensates. In addition to the familiar triangular lattice predicted by Tkachenko for  $^4\text{He}$ , many more complex lattices appear in this system as a result of the spin degree of freedom. In particular, we predict a magnetic-field-driven transition from a triangular lattice to a honeycomb lattice. Other transitions and lattice geometries are driven at constant field by changes in the temperature-dependent ratio of charge and spin stiffnesses, including a transition through an aperiodic vortex structure.

PACS numbers: 03.75.Mn

One of the many remarkable properties of superfluids is the appearance of vortex lattices in rotated systems [1, 2]. These lattices are periodic arrangements of vortices that allow the superflow outside the vortex cores to remain irrotational and are analogous to the mixed state of type-II superconductors in a magnetic field. Bose condensates of atoms with nonzero integer spin [3, 4, 5], referred to as “spinor Bose condensates”, combine spin and superfluid ordering in different ways depending on the spin and the interatomic interaction. These condensates, and the vortices and other topological defects that they allow, have been actively studied in recent years.

Since the physics of individual defects in spinor Bose condensates is now understood for the most experimentally relevant cases with total spin  $F \leq 3$ , [6, 7, 8, 9, 10, 11], a natural next step is to understand physical situations controlled by the collective physics of many defects. Two examples are the vortex lattice in a rotated condensate and the superfluid transition in a two-dimensional condensate. In general, the lowest-energy vortex defects of spinor condensates have both superfluid and spin character. Although external rotation of the condensate couples only to the superfluid part, the mixed nature of the vortices means that the interaction between the spin parts of different vortices is also important in determining the vortex lattice.

This letter uses a general approach to vortex lattice phases in spinor condensates, including the quadratic Zeeman anisotropy normally present in experimental systems, to show that the cyclic phase of an  $F = 2$  spinor condensate undergoes an unusual vortex lattice transition in a weak applied magnetic field. This transition allows collective physics resulting from the nontrivial spin configuration of vortices to be imaged using spin-insensitive measurements. The comparison of energies of different lattices uses an Ewald summation trick that exactly reproduces previous results obtained for simpler lattices using elliptic functions [1]. More generally, the methods of this letter allow the energy of any periodic

arrangement of vortices in a spin-anisotropic spinor condensate to be rapidly calculated. We also show that under some conditions there is a strictly aperiodic vortex structure rather than a true lattice.

Dilute  $F = 2$  bosons interact via the potential  $V(|\mathbf{r}_1 - \mathbf{r}_2|) = \delta(\mathbf{r}_1 - \mathbf{r}_2)(g_0 P_0 + g_2 P_2 + g_4 P_4)$ , where  $P_F$  projects into the total-spin  $F$  state and  $g_F = 4\pi\hbar^2 a_F/M$  determines  $g_F$  given  $a_F$ , the scattering length in the spin- $F$  channel. This two-body potential gives the interaction Hamiltonian [12, 13]

$$\mathcal{H}_{\text{int}} = \int d\mathbf{r} : \frac{\alpha}{2}(\psi^\dagger \psi)^2 + \frac{\beta}{2}|\psi^\dagger \mathbf{F} \psi|^2 + \frac{\tau}{2}|\psi^\dagger \psi_t|^2 :, \quad (1)$$

with  $\psi$  a five-component vector field whose component  $\psi_m(\mathbf{r})$  destroys a boson at point  $\mathbf{r}$  with  $F_z = m$ ,  $m = -2, \dots, +2$ , and  $\mathbf{F}$  denoting the spin-2 representation of the  $SU(2)$  generators.  $\psi_t$  is the time-reversal conjugate of  $\psi$ :  $\psi_{tm} = (-1)^m \psi_m^\dagger$ . The parameters in this Hamiltonian are determined by  $g_0, g_2, g_4$  via  $\alpha = (3g_4 + 4g_2)/7$ ,  $\beta = -(g_2 - g_4)/7$ ,  $\tau = \frac{1}{5}(g_0 - g_4) - \frac{2}{7}(g_2 - g_4)$ . To  $H_{\text{int}}$  must be added the one-body Hamiltonian for an isotropic and spatially uniform condensate

$$\mathcal{H}_0 = \int d\mathbf{r} \frac{\hbar^2}{2M} \nabla \psi^\dagger \cdot \nabla \psi - \mu \psi^\dagger \psi, \quad (2)$$

where  $\mu$ , the chemical potential. Minimizing this Hamiltonian over single-particle condensates leads to three phases: ferromagnetic, antiferromagnetic, and cyclic. The cyclic phase that will be the focus of our work occurs when  $\beta, \tau > 0$  and is expected to be realized in a condensate of  $^{85}\text{Rb}$  atoms [12]. The spinor structure of this state, having the symmetry of the tetrahedron, results in a nonabelian homotopy group which has been pursued in the liquid physics community for several years.

In all existing experiments, an important effect even at the single-particle level is the existence of anisotropy in spin space resulting from the magnetic fields used as part of the trapping process. Including the hyperfine interaction, the bosons we consider interact with the external

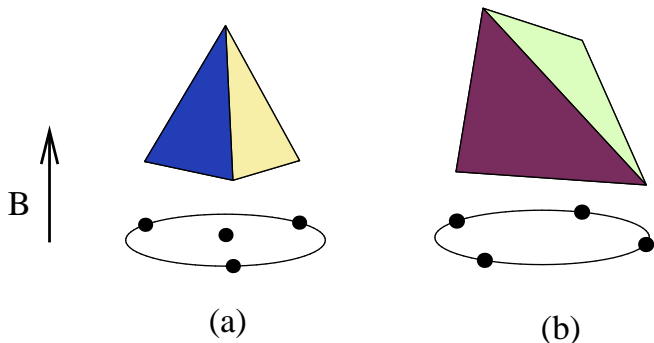


FIG. 1: Orientations of the cyclic state in an external magnetic field which breaks the spin rotational symmetry. Upon increasing the magnetic field, the spinor will undergo a transition from state (a) to state (b).

magnetic field as  $\mathcal{H}_z = \Gamma \mathbf{I} \cdot \mathbf{S} - 2\mu_B B_z$  where  $\Gamma$  is the magnitude of the hyperfine interaction,  $\mathbf{I}$  is the nuclear spin,  $\mathbf{S}$  is the electronic spin,  $\mu_B$  is the Bohr magneton, and  $B$  is the magnitude of the magnetic field taken to point in the  $z$ -direction. Within the manifold of spin-two states, a Hamiltonian which reproduces the correct energies up to a constant is given by  $\mathcal{H}_z = \sqrt{\Gamma^2 + (\mu_B B)^2} + \Gamma \mu_B B F_z$  [14]. This Hamiltonian can be expanded in powers of  $F_z$ . Since the relaxation time of the total magnetization is typically longer than the condensate lifetime, the linear term can be neglected. Particular attention has been paid to the next term which gives rise to the quadratic Zeeman effect [3]. However, due to the high symmetry of the cyclic state, this quadratic term alone is not enough to select its orientation. For this case, one therefore must consider the cubic term which is at next order.

To determine the spin states in the presence of such a magnetic field, one must also consider the spin exchange interaction energy of the condensate per particle which is  $E_s = \frac{1}{2}n\beta\langle\mathbf{F}\rangle \cdot \langle\mathbf{F}\rangle + \frac{1}{2}n\tau|\langle\chi|\chi_t\rangle|^2$ , where  $n$  is the condensate density. Since the total spin is assumed to be conserved in experiments, we can neglect the first term in this expression. Minimizing  $E_s + E_z$  (where  $E_z = \langle\mathcal{H}_z\rangle$ ) over possible spinor states we find the following: At small magnetic fields, the spinor  $\chi_{t1} = (\sqrt{1/3}, 0, 0, \sqrt{2/3}, 0)^T$  (up to any rotation about the  $z$ -axis) is selected. In the classification scheme described in [15], this state is represented by a tetrahedron with one of its faces parallel to the  $xy$  plane. Upon increasing the magnetic field there is a transition at  $\mu_B B_c = n\tau/16$  to the spin orientation  $\chi_{t2} = (\sin(\theta)/\sqrt{2}, 0, \cos(\theta), 0, -\sin(\theta)/\sqrt{2})^T$ , where  $\theta$  changes continuously with increasing magnetization. This spinor has the symmetries of a distorted tetrahedron with one of its edges parallel to the  $xy$  plane (when  $\theta = \pi/4$  it has the symmetries of the regular tetrahedron). These two types of orientations are summarized in Fig. 1. The magnitude of the critical field is of the

order of ambient fields in current experiments [16] but smaller fields can in principle be simulated by optical means [17].

Having identified the different types of tetrahedral states that are stabilized in an applied magnetic field, we now discuss the effects of rotation in addition to the applied field. The rotation couples to the phase of the condensate and has the effect of producing point vortices in two dimensions or lines of vortices in three dimensions. A vortex is a special type of configuration in an ordered phase that breaks a continuous symmetry: sufficiently far from a “core” region (linear in 3D or point-like in 2D) in which the order is destroyed. The configuration is locally in an ordered state, but cannot be smoothly deformed to the uniform configuration.

We find in general that vortices form a two-dimensional lattice whose properties depend on the nature of the constituent vortices and the interactions between them. For simplicity, it is assumed that the magnetic field and the axis of rotation are in the same direction. Owing to the  $\pi/3$  spin rotation symmetry of the state (a) that is stabilized at fields  $B < B_c$ , its vortices are of three types:  $(n, m)$ ,  $(n - 1/3, m + 1/3)$  and  $(n + 1/3, m - 1/3)$ , where  $n$  and  $m$  are integers and the first argument inside the parentheses is the winding number of the phase while the second is that of the spin. The vortex lattice that is formed has a net nonzero winding number for the phase and zero winding number for the spin.

The energetics, in addition to the above constraints on the winding numbers, will depend on the stiffnesses  $K_c$  and  $K_s$  of the condensate corresponding respectively to the charge (phase) and the spin. (The expected behavior of these stiffnesses will be discussed in closing.) The interaction energy of two vortices  $(x_1, y_1)$  and  $(x_2, y_2)$  separated by a distance  $r$  in the state (a) is given by

$$E = 2\pi K_c x_1 x_2 \log(\xi/r) + \pi K_s y_1 y_2 \log(\xi/r), \quad (3)$$

where  $\xi$  is the typical radius of a vortex. For  $K_s > K_c$ , it is energetically favorable to produce only vortices of the type  $(1, 0)$ . However, for  $K_s/K_c < 1$ , the  $(1, 0)$  vortex breaks up into  $(2/3, 1/3)$  and  $(1/3, -1/3)$  vortices as can be seen by putting the appropriate values of the winding numbers into Eqn. 3. Once again, the energetics are subject to the constraints of rotation mentioned in the previous paragraph. For values of  $K_s/K_c < 1/4$ , each  $(2/3, 1/3)$  vortex breaks up into  $(1/3, 2/3)$  and  $(1/3, -1/3)$  vortices. Thus, in this regime, there are only  $(1/3, 2/3)$  and  $(1/3, -1/3)$  vortices with twice as many of the latter as the former. Since, the nature of the vortices is determined by the ratio  $K_s/K_c$ , so too is the lattice they form as will be described later. For  $B > B_c$ , the state (b) is stabilized. This state can be shown to have vortices only of the type  $(n, m)$ . When subjected to a rotation only  $(1, 0)$  vortices will be produced like at low fields with  $K_s > K_c$ .

Thus, to summarize, the following kinds of vortices are produced by rotation: 1)  $(1, 0)$  vortices for  $K_s > K_c$  or  $B > B_c$ , 2) an equal number of  $(2/3, 1/3)$  and  $(1/3, -1/3)$  vortices for  $1/4 < K_s/K_c < 1$  and  $B < B_c$  and 3) twice as many  $(1/3, -1/3)$  vortices as  $(1/3, 2/3)$  for  $0 < K_s/K_c < 1/4$  and  $B < B_c$ . In each case, the density of vortices is determined by the angular velocity of the rotation.

Having determined the types of vortices that are produced at the various values of magnetic field and stiffnesses, we now evaluate the energies of vortex lattices. Due to the long-ranged nature of the logarithmic interactions, the energy of a vortex lattice is difficult to evaluate directly. Thus, we develop a method that is similar to the Ewald summation technique for the cohesive energy of three-dimensional ionic crystals [18, 19]. For simplicity, we use a scalar condensate to demonstrate the technique; the generalization to spinor condensates is straightforward and will be given presently. The energy (in units of the stiffness) of a single vortex taken to be at the origin is given by

$$\phi(0) = \sum_{\mathbf{R} \neq 0} \log \left( \frac{\xi}{\mathbf{R}} \right) - \int d^2r \rho_0 \log \left( \frac{\xi}{r} \right), \quad (4)$$

where  $\mathbf{R}$  are the lattice vectors and  $\xi$ , the size of the vortex. The second term is due to a uniform negative background charge of density  $\rho_0$  which arises from the fact we are working in a rotating frame of reference. Note that each of these terms diverges individually but their difference does not. The Ewald trick is to add and subtract a normalized Gaussian function  $\frac{1}{\pi\sigma^2} e^{-r^2/\sigma^2}$  from each point charge, where  $\sigma$  is a screening length. For instance, the potential of a point charge at the origin screened by such a Gaussian function is  $\phi(r) = \frac{1}{2} \text{Ei}(r^2/\sigma^2)$ , where  $\text{Ei}(x) = \int_x^\infty dt e^{-t}/t$  is the exponential integral. Note that this will decay exponentially fast at large distances. In three dimensions the corresponding potential is  $\phi(r) = (1 - \text{erf}(r))/r$  where  $\text{erf}$  is the error function.

Proceeding along these lines, the resulting potential corresponding to Eq. 4 is

$$\begin{aligned} \phi(0) = & \frac{1}{2} \sum_{\mathbf{R} \neq 0} \text{Ei} \left( \frac{R^2}{\sigma^2} \right) + \sum_{\mathbf{G} \neq 0} \rho_0 \frac{2\pi}{G^2} e^{-\frac{\sigma^2}{4} G^2} \\ & - \log \left( \frac{\xi}{\sigma} \right) - \frac{\gamma}{2} - \rho_0 \frac{\pi}{2} \sigma^2, \end{aligned} \quad (5)$$

where  $\mathbf{G}$  are the reciprocal lattice vectors and  $\gamma$  is the Euler-Mascheroni constant. The first term comes from the density of point charges screened by the Gaussian function while second term comes from difference of the charge density of the Gaussian functions and the uniform charge density. The term  $-\log \left( \frac{\xi}{\sigma} \right) - \frac{\gamma}{2}$  is obtained after subtracting off the additional Gaussian function at the origin where we omit the charge. Finally, the last term is

to make the average of the screened potential zero [19]. On the other hand, the potential of a test charge away by  $\mathbf{d}$  from the origin is

$$\begin{aligned} \phi(\mathbf{d}) = & \frac{1}{2} \sum_{\mathbf{R}} \text{Ei} \left( \frac{|\mathbf{R} - \mathbf{d}|^2}{\sigma^2} \right) + \sum_{\mathbf{G} \neq 0} \rho_0 \frac{2\pi}{G^2} e^{-\frac{\sigma^2}{4} G^2} e^{i\mathbf{G} \cdot \mathbf{d}} \\ & - \rho_0 \frac{\pi}{2} \sigma^2 \end{aligned} \quad (6)$$

The best check of this procedure is to see if the sum is independent of the parameter  $\sigma$ . The two sums in real and reciprocal space in Eqns. 5 and 6 both converge exponentially fast. In this way, the energy per vortex of the square lattice is found to be  $\phi_s(0) = -\log \left( \frac{\xi}{a} \right) - 1.3105$  (where  $a$  is the lattice constant) while that of the triangular lattice at the same density is found to be  $\phi_t(0) = -\log \left( \frac{\xi}{a} \right) - 1.3211$ . Both are in precise agreement with the results obtained by integrating over the full spatial flow pattern [1]. For vortices in spinor condensates, which contain windings of phase and spin, the above procedure is applied individually to each sector with the Ewald sums being weighted by the corresponding stiffnesses. The main advantage of the Ewald technique is that it can be generalized to treat complicated unit cells with an arbitrary number of vortices in them in a straightforward and numerically efficient manner.

Let us first consider the case  $B > B_c$ . As noted earlier, the vortices produced by the rotation are of the type  $(1, 0)$ . These form the usual triangular lattice for all values of  $K_s/K_c$ . For  $B < B_c$ , the fractional winding numbers of the fundamental vortices give rise to more interesting possibilities. For  $1/4 < K_s/K_c < 1$ , the lattice is bipartite with equal numbers of  $(2/3, 1/3)$  and  $(1/3, -1/3)$  vortices. We use the Ewald summation technique to numerically evaluate the energy of the lattice assuming the same parallelogram unit cell for both sublattices and an arbitrary displacement between them. We then perform a minimization of the energy over these parameters to identify the lattice that is produced at different values of  $K_s/K_c$ . The sequence of lattices is described in Fig. 2. At exactly  $K_s/K_c = 1$ , the two sublattices do not interact with each other and each is a triangular lattice. As soon as  $K_s/K_c$  is lowered and the two begin to interact, the honeycomb lattice is stabilized and remains so till  $K_s/K_c = 0.76$ . Below this value, the vortices of one type move to the centers of the rhombic unit cells formed by the other type which we term an interpenetrating rhombic lattice. The internal angle of the rhombus changes continuously with  $K_s/K_c$  from  $\pi/3$  at  $K_s/K_c = 0.76$  to  $\pi/2$  at  $K_s/K_c = 0.64$ . The interpenetrating square lattice thus obtained at  $K_s/K_c = 0.64$  is stable down to  $K_s/K_c = 1/4$ . This sequence of lattices is the same as obtained for rotating two-component condensates in the quantum Hall regime [20], or equivalently the  $F = 1$  polar condensate, but the values where the transitions occur are different for  $F = 2$ .

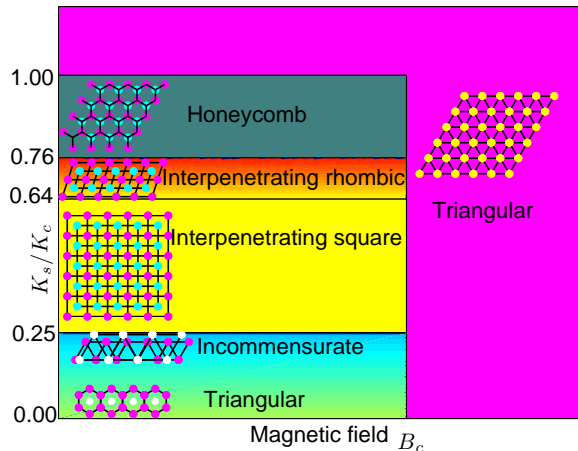


FIG. 2: A schematic depiction of the different types of vortex lattices obtained at different values of  $K_s/K_c$  and magnetic field. The color code for the vortices is:  $(1,0)$  yellow,  $(2/3,1/3)$  cyan,  $(1/3,-1/3)$  magenta and  $(1/3, -2/3)$  white.

For  $K_s/K_c < 1/4$ , a lattice with  $(1/3, 2/3)$  and  $(1/3, -1/3)$  vortices is obtained with twice as many of the latter as the former. Exactly at  $K_s/K_c = 1/4$ , the two sublattices do not interact and each is a triangular lattice. The sublattice of the  $(1/3, 2/3)$  vortices has a unit cell of length  $\sqrt{2}$  times that of the  $(1/3, -1/3)$  vortices. These two lattices are *incommensurate* for any rotation angle between them, which follows from showing that the nonzero squared lengths of lattice vectors in one lattice are disjoint from those in the other lattice. This incommensurability implies that the energy of interaction between the two lattices can be calculated using the Ewald technique by averaging over all displacement vectors instead of specific lattice points, and the result is zero. In the other limit,  $K_s/K_c \rightarrow 0$ , the interaction between all pairs of vortices is identical and a triangular lattice is obtained. While there are several way to distribute the two kinds of vortices in such a lattice, the lattice where the  $(1/3, -1/3)$  vortices form a honeycomb lattice while the  $(1/3, 2/3)$  vortices are at the centers of each hexagon is the most symmetric one with three vortices per unit cell. The behavior between the incommensurate structure at  $K_s/K_c = 1/4$  and this specific triangular structure as  $K_s/K_c \rightarrow 0$  is difficult to determine reliably by our technique, since given the existence of the incommensurate structure, there is no justification for a numerical search over unit cells with a finite number of basis vectors.

As demonstrated above, transitions between different vortex lattices can be tuned by a magnetic field  $B$  or the ratio  $K_s/K_c$ . While the field  $B$  can be applied directly or its effect simulated through optical techniques in experiments [17], the ratio  $K_s/K_c$  is more difficult to manipulate directly. In spinor condensates at low temperatures,

this ratio is typically close to 1 but is renormalized by quantum and thermal fluctuations. Increasing temperature acts to reduce  $K_s$  more rapidly than  $K_c$ , because the soft spin modes that are excited at finite temperature have a larger phase space than the phase modes (assuming that the quadratic Zeeman term can be neglected). Both a nonlinear-sigma-model analysis and a study of Bogoliubov-like excitations suggest that under normal experimental conditions at nonzero temperature,  $K_s$  is slightly less than  $K_c$  so that the magnetic transition will be observable. The best possibility to observe evolving vortex structure as  $K_s/K_c$  is further reduced is to raise the temperature very close to  $T_c$  of the condensate: if the magnetic order is lost before the superfluid order, as allowed by Landau theory, this ratio will rapidly decrease to zero in a narrow temperature range.

To conclude, we have shown using the Ewald summation technique that different types of vortex lattices can be produced in cyclic condensates as functions of magnetic field and the ratio of the charge and the spin stiffnesses. In particular, there is a magnetic-field-driven transition from a triangular to a honeycomb lattice. In the low-field limit, there are both abrupt transitions and continuous families of lattices as functions of the ratio of the stiffnesses, including the appearance of an incommensurate structure at one value.

The authors would like to thank D. A. Huse, M. Lucianovic, O. Motrunich, D. Podolsky, D. Stamper-Kurn, M. Vengalattore, and A. Vishwanath for useful discussions. RB was supported by the Sherman Fairchild Foundation, SM by DOE/LBNL, and JEM by NSF DMR-0238760.

- 
- [1] V. Tkachenko, Soviet Phys. JETP **22**, 1282 (1966).
  - [2] E. J. Yarmchuk, M. J. V. Gordon, and R. E. Packard, Phys. Rev. Lett. **43**, 214 (1979).
  - [3] J. Stenger, S. Inouye, D. M. Stamper-Kurn, H. J. Miesner, A. P. Chikkatur, and W. Ketterle, Nature **396**, 345 (1998).
  - [4] T. L. Ho, Phys. Rev. Lett. **81**, 742 (1998).
  - [5] T. Ohmi and K. Machida, J. Phys. Soc. Japan **67**, 1822 (1998).
  - [6] F. Zhou, Phys. Rev. Lett. **87**, 080401 (2001).
  - [7] H. Mäkelä, J. Phys. A.: Math. Gen. **39**, 7423 (2006).
  - [8] S. Mukerjee, X. Xu, and J. E. Moore, Phys. Rev. Lett. **97**, 120406 (2006).
  - [9] G. Semenoff and F. Zhou, Phys. Rev. Lett. **98**, 100401 (2007).
  - [10] S. K. Yip, Phys. Rev. A **75** (2007).
  - [11] R. Barnett, A. Turner, and E. Demler, Phys. Rev. A **76**, 013605 (2007).
  - [12] C. V. Ciobanu, S. K. Yip, and T. L. Ho, Phys. Rev. A **61**, 033607 (2000).
  - [13] M. Ueda and M. Koashi, Phys. Rev. A **65**, 063602 (2002).
  - [14] G. Briet and I. I. Rabi, Phys. Rev. **38**, 2082 (1931).
  - [15] R. Barnett, A. Turner, and E. Demler, Phys. Rev. Lett.

- 97**, 180412 (2006).
- [16] L. E. Sadler, J. M. Higbie, S. R. Leslie, M. Vengalattore, and D. M. Stamper-Kurn, *Nature* **443**, 312 (2006).
- [17] F. Gerbier, A. Widera, A. Foelling, O. Mandel, and I. Bloch, *Phys. Rev. A* **73**, 041602(R) (2006).
- [18] P. Ewald, *Ann. Phys.* **64**, 253 (1921).
- [19] M. P. Tosi, *Solid State Phys.* **16**, 107 (1964).
- [20] E. J. Mueller and T. L. Ho, *Phys. Rev. Lett.* **88**, 180403 (2002).